Kovove Mater. 54 2016 429–440
DOI: 10.4149/km_2016_6_429

High-temperature compression of closed cell aluminium foams

J. Kováčik*, Ľ. Orovčík, J. Jerz

Institute of Materials and Machine Mechanics, Slovak Academy of Sciences, Dúbravská cesta 9, 845 13 Bratislava, Slovak Republic

Received 10 June 2016, received in revised form 23 September 2016, accepted 26 September 2016

Abstract

The compression behaviour of closed cell aluminium foams (Al99.5, AlMg1Si0.6 and AlSi12 matrix alloys, TiH_2 foaming agent) prepared by powder metallurgy was studied in the temperature range of 20–550 °C. It was observed that the temperature increase results in the decrease of the compression strength and energy absorption and increase of densification strain (plateau length) at constant density. The dependence of compression strength on foam density and temperature was successfully modelled using new proposed equation. The activation energy for compression of aluminium foams seems to be density dependent with a maximum at certain density range depending on foam composition. It was also found that the characteristic exponent T_f for the compression strength of aluminium foams is temperature dependent variable. The strain at compression strength (deformation up to the macroscopic failure of foam) is nearly temperature independent or decreases at constant density depending on aluminium alloy matrix. The absorbed energy per unit volume of aluminium foams decreases with increasing temperature significantly due to the decrease in the value of plateau/compression strength at constant density.

K e y w o r d s: aluminium foam, powder metallurgy, compression, temperature, strength, energy absorption

1. Introduction

While the mechanical behaviour of cellular metallic materials prepared by powder metallurgy at room temperature has been widely studied in recent years [1–5], only a few studies concerning temperature dependence of foams in compression have been performed since pioneering work of Thornton and Magee [6]. They studied zinc foams compression behaviour in the temperature range from –196 up to 200 °C.

The most of the foams applications now exist only at room temperatures. For example, industrial applications developed at IMMM SAS Bratislava from PM aluminium foams are following: stiffener of side rail in Ferrari Modena 360 (6,000 pcs year^{-1}), crash box against rare impact in Audi Q7 (120,000 pcs year^{-1}) and bumper of railway carriages in Siemens and Bombardier light trains (1,000 pcs year^{-1}) [7].

Why is the temperature effect on compression behaviour of foams so important? Because there are a number of applications of metallic foams in which elevated temperatures are involved: Open cell foams are used in heat exchangers or as catalyst carriers in chemical reactors. Closed cell foams are used as core materials in lightweight components and aluminium castings in automotive and aerospace constructions, where elevated or high temperatures frequently exist next to combustion or propellant engines. Moreover, considering possible using of aluminium foams in buildings it is necessary to know also its compression behaviour at elevated temperatures during accidental fires.

It has been already observed that the testing temperature changes the mechanical properties of metal foams [8–11]. Compressive tests at different temperatures (25–620 °C) were performed on closed cell Alporas foams [8]. The results indicated that the mechanical properties of Al-foams were strongly dependent on the density of foams as well as testing temperature. Buckling of cell walls was the dominant deformation mechanism [8]. Compressive properties at 300–500 °C of aluminium foams produced by the spacer method were also investigated [9]. The stress expo-

*Corresponding author: e-mail address: Jaroslav.Kovacik@savba.sk

nent and activation energy for deformation at elevated temperatures in the Al foams were in agreement with those in the bulk Al alloy [9]. The dynamic compressive behaviour of aluminium foams was investigated at different temperatures [10]. It showed that the dynamic deformation process possesses more fragments and debris spilled out at room temperature. At elevated temperature, the deformation mainly results from the plastic bending of the cell wall. Compressive deformation behaviour of ZA27 foams has been studied at varying temperatures from 100 to 250 °C [11]. It was observed that plateau stress and energy absorption increase with increasing relative density and strain rate, and decrease with increasing temperature [11].

The research mentioned above was mainly focused on ductile metal foams. In the work of Liu et al. [12] the compressive properties of Al-Si-SiC brittle composite foams at different temperatures were studied from room temperature (25 °C) to elevated temperature (200 and 400 °C). They observed brittle-type fracture mode at room temperature, but when the testing temperature increased up to 400 °C, the ductile-type fracture mode occurred. This indicates the softening effect of temperature on foam matrix.

The aim of the present work is to study systematically the temperature effect on the deformation behaviour of PM closed cell aluminium foams made from different metal matrix from room temperature up to 550 °C. Both ductile and brittle metal matrix alloys will be used in this study.

2. Experimental

The aluminium foams examined in this study were made from three matrix compositions: pure Al99.5, wrought AlMg1Si0.6 alloy and casting brittle AlSi12 aluminium alloy. Aluminium foams Alulight were prepared by powder metallurgical route at the Institute of Materials and Machine Mechanics, Bratislava using 0.4 wt.% of TiH_2 as a foaming agent. As-prepared foam samples with surface skin (geometry $28 \times 70 \times 500\,mm^3$, see Fig. 1) were cut into samples without skin (geometry $28 \times 25 \times 25\,mm^3$) using electric discharge machine. The density of cut samples was typically found in the range of 300–700 $kg\,m^{-3}$. The samples with the same density were selected for temperature experiments to eliminate the effect of structure on the compression behaviour of foams. The following heat treatment was used to clean all samples after electric discharge cutting: heating of samples (2 °C min^{-1}) followed by 1-hour dwell at 500 °C and then cooling (4 °C min^{-1}) down to the room temperature.

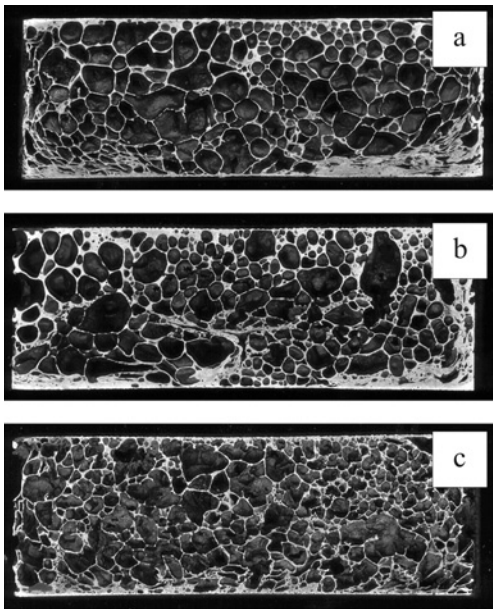

Fig. 1. As-prepared aluminium foam structures (cross section of $28 \times 70\,mm^2$): (a) Al99.5 – overall density 540 $kg\,m^{-3}$, (b) AlMg1Si0.6 – overall density 540 $kg\,m^{-3}$, (c) AlSi12 – overall density 610 $kg\,m^{-3}$.

Table 1. Composition, melting temperature, density range, temperature and number of aluminium foam samples used in this study, T_m is melting temperature of used alloy

Alloy	Al99.5		AlSi12		AlMg1Si0.6	
T_m (°C)	660		580–590		650–660	
Test temperature (°C)	Density range ($kg\,m^{-3}$)	No. of samples (–)	Density range ($kg\,m^{-3}$)	No. of samples (–)	Density range ($kg\,m^{-3}$)	No. of samples (–)
20	310–560	8	410–820	8	380–650	7
100	–	–	720	1	405	1
200	300	1	730	1	433	1
300	280–500	8	400–720	7	400–530	7
400	310	1	730	1	411	1
500	320–560	11	430–720	11	425-550	9
550	330	1	–	–	420	1

The samples were tested on 10 kN ESH servohydraulic testing machine (ESH 2094, ESH testing Ltd., UK) with constant crosshead speed 5 mm min^{-1} at the Department of Materials Science and Metallurgy, Cambridge. See Table 1 for a complete list of samples density and testing temperatures. A computer controlled infrared oven was used to heat up the samples up to 100, 200, 300, 400, 500 and 550 °C. The heating rate was 5 °C min^{-1}. Because controlling thermocouple cannot be placed within foam during the experiment, it was placed just beside sample in a piece of bulk copper. The temperature stabilisation inside foam was checked using a reference AlSi12 foam sample prior all experiments, as AlSi12 alloy foam possesses the lowest thermal conductivity from all used alloys. During calibration, the thermocouple was positioned in the centre of the reference sample. After heating to the desired temperature, the sample was held at this temperature for 15 min before the compression test was started. To check the validity of this approach the compression tests at 500 °C were also performed 5 min before, at 10 and 15 min after this optimal time for all three investigated alloys. No influence on the compression behaviour of foams was observed thus confirming the accuracy of chosen 15 min dwell on temperature to reach the desired foam temperature.

Finally, the stress-strain curves were created, and compression strength, strain at compression strength, plateau length, densification strain and energy absorption were evaluated for each sample according to usual approaches [13].

3. Results and discussion

Figures 2–4 illustrate the effect of the temperature on the compression stress-strain curves of investigated aluminium foams at constant density and strain rate of 3×10^{-3} s^{-1}. At room temperature, the mechanical and physical properties of aluminium foams depend predominantly on the corresponding property of bulk metal or metal alloy from which the foam is prepared, and foam porosity. The properties of the foam are further influenced by the anisotropy and heterogeneity of foam structure; and also by the presence of imperfections [14] within foam cell walls: cracks, voids, kinks and wiggles.

There are two basic deformation mechanisms of aluminium foams that depend on the type of used aluminium alloy: brittle fracture and ductile failure. They were primarily studied by the microstructure investigation of fractured foam cell walls in tension [15]: AlSi12 foam fails by a mixture of ductile tearing and cleavage fracture while AlMg1Si0.6 foam by ductile void growth. In compression, casting aluminium alloy foams exhibit usually brittle fracture and bulk aluminium and wrought aluminium alloys exhibit plastic

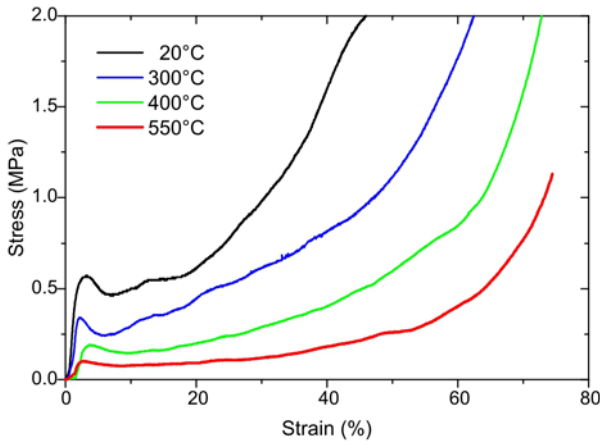

Fig. 2. Temperature dependence of stress-strain curves: Al99.5 aluminium foams, density 308 ± 19 kg m^{-3}.

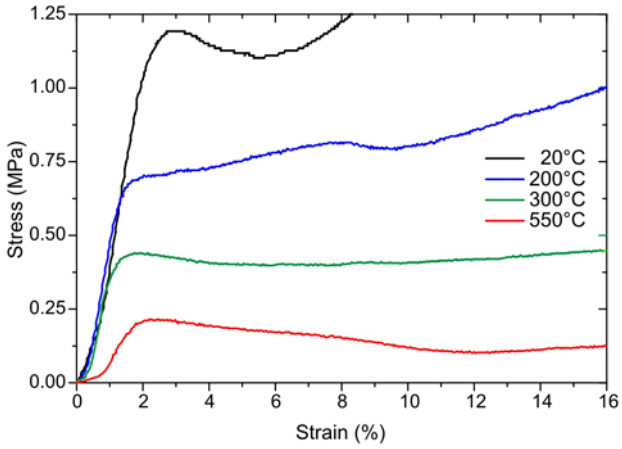

Fig. 3. Dependence of the elastic-plastic region and the beginning of the plateau on the temperature for AlMg1Si0.6 aluminium foams at constant density 412 ± 15 kg m^{-3}.

collapse of the whole sample at the weakest link of the structure.

Later the brittle failure of the cell walls in the pore layers neighbouring to the previously fractured layer (cracks grow) leads to multiple stress drops and to the serrated stress-strain curve in the plateau region (Fig. 4). The strain magnitude of the first stress drop depends on the average pore size of the foam structure [16].

On the contrary for ductile alloys, the following plastic buckling of almost all cell walls leads to the subsequent lateral expansion of the whole foam sample again and again via weakest links, which results in the smooth plateau region (Figs. 2–3). At higher porosities, the first stress drop can also be observed for pure Al and wrought aluminium alloy foams due to increased foam heterogeneity.

At high temperature, the density, macrostructure and structural imperfections within cell walls of foam remain almost unchanged. Therefore the foam prop-

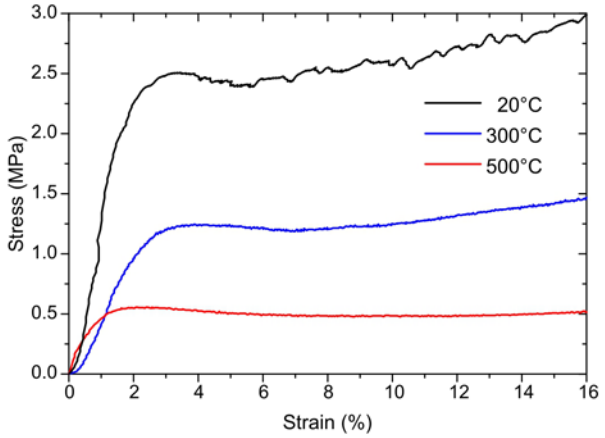

Fig. 4. Dependence of the elastic-brittle/plastic region and the beginning of the plateau on the temperature for AlSi12 aluminium foams at constant density 465 ± 8 kg m^{-3}.

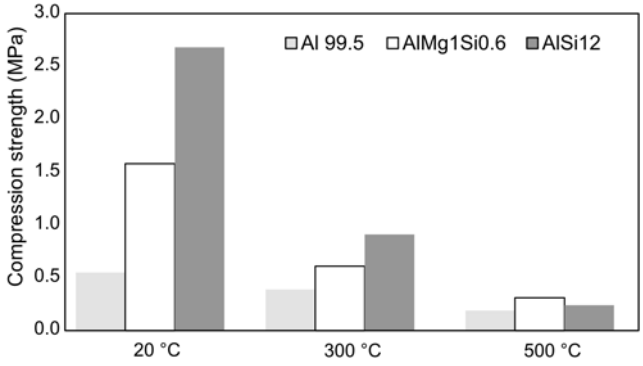

Fig. 5. The comparison of the compression strength of different aluminium foams at various temperatures (density 480 kg m^{-3}).

erties with increasing temperature are principally determined by the properties of the metal alloys at given temperature. For ductile aluminium alloys at temperatures above $0.3T_m$ the thermal energy is sufficient to permit dislocations to climb as well as glide, bypassing obstacles which hold them up [13]. The mechanisms possible at high temperature are a power-law creep, diffusional flow and metal recrystallisation.

As the temperature of brittle alloys is raised above $0.3T_m$ the deformation causes holes to nucleate at inclusions; plastic strain makes them grow and coalesce to give ductile failure. This effect leads to the enhanced ductility of brittle AlSi12 foam (see Fig. 4), and serrated stress-strain curve at 20 °C is altered to smooth stress-strain curve at and above 300 °C. In this case, the mechanisms possible at the high temperature are a power-law creep and dynamic recrystallization.

With increasing temperature, the compression strength and plateau stress of aluminium foams decrease significantly. The heating up above 300 °C also diminishes the differences between compression strength of various aluminium alloy foams significantly (see Fig. 5). This is in good agreement with tensile strength behaviour of various aluminium alloys at higher temperatures. It also confirms that the thermal strengthening of aluminium foams [17] will disappear after sufficient dwelling at high temperature.

It must be pointed out that it is difficult for solid metal alloys to determine the precise value of compression strength. Therefore further in the article, the ultimate tensile strength of bulk metal alloy is usually considered to describe/model compression strength of corresponding foams.

The compression strength σ_{cs} (stress at which the macroscopic failure of the sample occurs) and plateau stress of metallic foams are very important in the design of cushions, packaging and systems for energy absorption where foam strength plays a dominant role. The compression strength of a metallic foam depends on the compression strength of solid metal from which the foam is made, foam density, foam structure, applied strain rate [13] and of course on temperature.

It is generally accepted and experimentally confirmed that at room temperature, the density dependence of compression strength of foam can be characterised by power law equation [4, 13]:

$$\sigma_{cs}(\rho) = \sigma_{cs}\left(\frac{\rho}{\rho_s}\right)^{T_f}, \tag{1}$$

where $\sigma_{cs}(\rho)$ and ρ are the compression strength and the density of the foam, σ_{cs} and ρ_s is the compression strength and the density of the solid material from which the foam is made, respectively. T_f is the characteristic exponent for compression strength, and for aluminium foams usually belongs to the range of 1.8–2.1 [4].

Concerning temperature alteration of foam compression strength, all parameters in Eq. (1) – σ_{cs}, ρ, ρ_s and T_f – can be considered as temperature dependent. Fortunately, this complex problem can be reduced to the simple temperature dependence of compression strength of the solid material: If there is no phase transition in the metal matrix the characteristic exponent can be considered as temperature independent and the temperature dependence of metal volume fraction can be neglected.

To model the temperature dependence of compression strength of the solid metal a phenomenological equation usually utilised to describe compression behaviour of superalloys [18] at high temperature ($T > 0.3T_m$) can be used. It is the dependence between compression strength σ_{cs}, strain rate $\dot{\varepsilon}$ and temperature T of metals:

$$\sigma_{cs} = \sigma_s(0)\left(\frac{\dot{\varepsilon}}{A}\right)^{1/n_s} \exp\frac{Q_S}{n_s RT}, \tag{2}$$

Table 2. The activation energy and power law creep exponent [20] for 6101-T6 aluminium alloy open cell foams – Duocel, nominal pore size approximately 2 mm

Density (kg m^{-3})	2700	170	230	360
Q_S (kJ mol^{-1})	173	157	203	186
n_s (–)	4.0	4.8	4.2	3.5
Q_S/n_s (kJ mol^{-1})	43.3	32.7	48.3	53.1
T (°C)	275–325		275–350	

Table 3. The activation energy and power law creep exponent for pure aluminium [22]

	Grain boundary diffusion	Lattice diffusion
Q_S (kJ mol^{-1})	84	142
	dislocation creep ($T > 200$ °C)	
n_s (–)	4.4	4.4
Q_S/n_s (kJ mol^{-1})	19	32

where A, n_s and $\sigma_s(0)$ are constants, Q_S is the activation energy for the deformation process, and R is universal gas constant, $R = 8.3145\,\mathrm{J\,mol^{-1}\,K^{-1}}$. This model is consistent with the temperature dependence of yield stress of the solid material in Gibson and Ashby book [13].

The combination of Eqs. (1) and (2) gives the phenomenological model for the compression strength of metallic foam in the high-temperature region ($T > 0.3\,T_m$):

$$\sigma_{cs}(\rho, T) = \sigma_s(0)\left(\frac{\dot{\varepsilon}}{A}\right)^{1/n_s}\left(\frac{\rho}{\rho_s}\right)^{T_f}\exp\frac{Q_S}{n_s RT}, \quad (3)$$

where A, n_s and $\sigma_s(0)$ are constants, Q_S is the activation energy for the foam compression, and R is universal gas constant.

It must be pointed out, that constants in Eq. (3) seem to be creep constants on the first sight, but they are in reality phenomenological constants for compression. Under some conditions there exists certain equivalence between constant creep tests and constant strain rate deformation tests for aluminium and its alloys. Mecking et al. [19] showed that this equivalence holds if time-dependent processes, such as static recovery, ageing and grain coarsening for low strain rates in compression and precipitation in situ for creep at long times, do not influence significantly microstructure responsible for the deformation. Compression tests strain rate performed in this work was significantly high ($3 \times 10^{-3}\,\mathrm{s^{-1}}$) so it can be expected that time dependent processes are negligible and with some errors it is possible to discuss the obtained results using creep test results on aluminium and aluminium foams.

In the case of a compression test, the activation energy and power law creep exponent cannot be evaluated separately from the results, so it is necessary to look after the ratio of Q_S/n_s. As can be seen from Table 2, the experimentally obtained ratios of Q_S/n_s for nearly pure Al foam are similar to the same ratio for pure aluminium for lattice diffusion 32 kJ mol^{-1} (see Table 3). This confirms the assumption that foams should have the same activation energy and power law creep exponent as the solid material from which it is made and is consistent with the Andrews et al. [20] results for 6101-T6 aluminium alloy open cell foams (Table 2). However, the activation energy and power law creep exponent for closed cell Al-Si-Fe-Ti-Ca aluminium foam (density 240 kg m^{-3}) – Alporas [20] possess significantly different values below and above 300 °C.

The results for the cast and wrought alloy foams are a bit different, but it cannot be expected that the activation energy of pure aluminium and aluminium alloys is the same. Also creep stress exponent n_s can vary from 4 up to 12 or even more [21] depending on the aluminium alloy composition because not only usual mechanisms, such as dislocation gliding and climbing but also the precipitation hardening or dispersion strengthening can take place. Investigated powder metallurgical foams always consist of impurities, oxides (usually up to 2 wt.% of oxygen [15]), complex phases, cracks, and dissoluble Ti and Si particles. Due to this fact, AlSi12 foam (usually has a lot of cracks and contains a high amount of insoluble Si particles) possesses the highest investigated ratios of Q_S/n_s. Since various creep mechanisms can be present in the pure metal or alloy at given temperature, also the overall activation energy can be temperature dependent thus leading to non-linear dependence of the compression strength on the temperature for various aluminium alloy foams (see Fig. 6).

On the first sight the obtained values of Q_S/n_s seem to be significantly density dependent, but closer examination of the results confirmed that the fundamental differences between results are mainly due to the corresponding temperature range: For given alloy foam, the lowest ratio of Q_S/n_s is usually observed for data in the temperature range of 200–550 °C. The results for the data at {300 °C, 500 °C} are more similar at different densities (see Table 4 and Fig. 7). It also

Table 4. Linear regression results of Eq. (3) in the form $\log\sigma = C + \frac{1}{T}D$ for aluminium alloy foams. C and D are fitting constants, R' is correlation coefficient, and P is the number of data points

Alloy	Density (kg m^{-3})	C	D	R'	P	Q_S/n_s (kJ mol^{-1})
AlSi12 foam	**730***	−1.0492 ± 0.2568	891.62 ± 152.15	0.972	4	**17.1**
	520	−2.0196 ± 0.2730	1349.3 ± 177.70	0.967	6	25.8
	440	−2.0722 ± 0.4739	1244.5 ± 308.48	0.896	6	23.8
AlMg1Si0.6 foam	530	−1.3606 ± 0.1985	783.58 ± 129.20	0.974	4	15.0
	470	−1.5766 ± 0.2330	843.85 ± 159.58	0.894	9	16.2
	410*	−1.1160 ± 0.3095	486.60 ± 189.98	0.788	6	**9.3**
Al99.5 foam	470	−2.0794 ± 0.5105	1021.1 ± 325.61	0.814	7	19.6
	370	−2.0705 ± 0.2358	808.92 ± 153.50	0.935	6	15.5
	310*	−1.7451 ± 0.1828	674.15 ± 113.95	0.960	5	**12.9**

*Data in the range of 200–550 °C. **Other results are linear regression constants for data at {300 °C, 500 °C}.

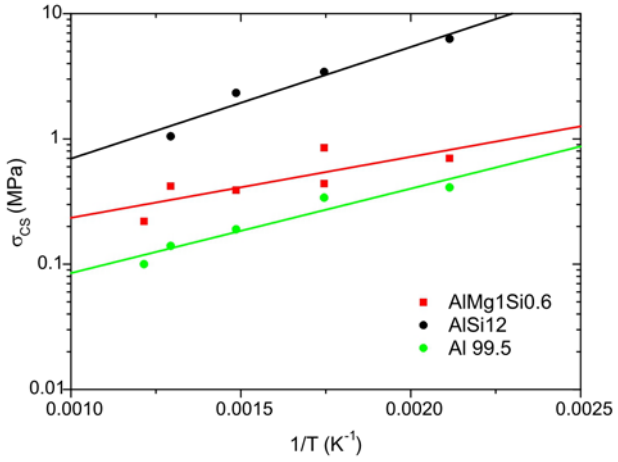

Fig. 6. The plot of compression strength versus temperature for aluminium alloy foams: AlMg1Si0.6 density 410 kg m^{-3}, AlSi12 density 730 kg m^{-3}, Al 99.5 density 310 kg m^{-3}, $T > 400$ K and linear regression lines.

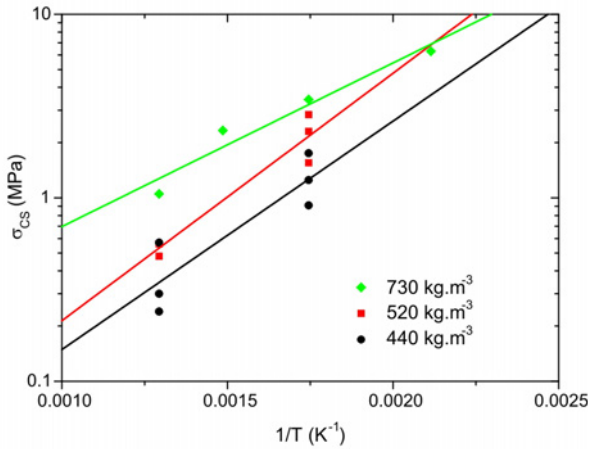

Fig. 7. The plot of compression strength versus temperature for AlSi12 aluminium alloy foams at various density, $T > 400$ K. Linear regression results are listed in Table 4.

confirms that at given temperature, the foam and solid material creep constants (activation energy, power law exponent) ought to be nearly the same regardless of the density.

Unfortunately, the situation is more complex in the case of foams. Andrews et al. [20] during studying of closed cell Alporas foam (see Table 5) showed that the creep exponent of foams depends on applied stress at a constant temperature. They suggested the following mechanism: At given load, due to the inhomogeneities in foam structure locally elevated stresses are sufficient to cause some cell walls to enter power law breakdown regime. These cell walls effectively shed their load to neighbouring cells acting as if they will be removed from the structure. At given temperature, there exists certain threshold stress value for this breakdown regime. If an external load is above the threshold stress, the creep exponent increases significantly.

Investigated PM closed cell foams usually possess more or less uniform structure, thus enabling some cell walls to enter power law breakdown regime at early stages of applied load. The foam structure is also significantly density dependent: with increasing porosity increases the average pore size, the presence of imperfections within foam cell walls (cracks, voids) and decreases the thickness of cell walls. Therefore the threshold stress value ought to vary with the foam density, thus more or less influencing the ratio of Q_S/n_s.

When the temperature rises, the synergetic effect of the microstructure of basic alloy and structure of foam made from this alloy takes place: During the creep at high temperature, the key role for bulk material plays the microstructure. In the case of the foam, the creep mechanisms of metal at microscale control the time evolution of the local stress distribution in cellular macrostructure, at given temperature. But the foam possesses random structure, where the small local stress alterations cannot be averaged out, thus leading to the substantial changes in the foam's load

Table 5. The activation energy and power law creep exponent [20] for closed cell Al-Si-Fe-Ti-Ca aluminium foam (density 240 kg m^{-3}) – Alporas, average cell size 4.5 mm

T (℃)	260–300	300–360	260–300	300–360
Q_S (kJ mol^{-1})	62.4	555.4	62.4	555.4
σ_{ext} (MPa)	0.25–0.42		0.42–0.68	
n_s (–)	5.4		15.0	
Q_S/n_s (kJ mol^{-1})	11.6	102.9	4.2	37.0

Table 6. Fitting results for strength-density dependence of various aluminium alloy foams according to Eq. (1) at a constant temperature; $\sigma_{cs}(T)$ is the compression strength of solid metal at given temperature; T_f is a characteristic exponent for the compression strength of aluminium foam at a constant temperature; $T_f(20\,℃)$ is an exponent at 20 ℃; χ^2 is minimisation function, and P is the number of data points

Alloy	T (℃)	$\sigma_{cs}(T)$ (MPa)	T_f (–)	$T_f - T_f(20\,℃)$ (–)	χ^2 (–)	P (–)
AlSi12	20	300.0 ± 1.0	2.74 ± 0.05	0	0.979	8
	300	45.0 ± 0.5	1.90 ± 0.05	–0.84	0.211	7
	500	12.3 ± 6.8	1.95 ± 0.38	–0.79	0.014	11
AlMg1Si0.6	20	110.0 ± 0.4	2.41 ± 0.05	0	0.171	7
	300	24.2 ± 43.5	1.93 ± 1.05	–0.48	0.039	7
	500	2.3 ± 4.1	1.06 ± 1.05	–1.35	0.007	9
Al99.5	20	70.0 ± 0.3	2.50 ± 0.08	0	0.088	8
	300	20.0 ± 0.1	2.12 ± 0.07	–0.38	0.018	8
	500	1.8 ± 2.2	1.36 ± 0.71	–1.14	0.004	11

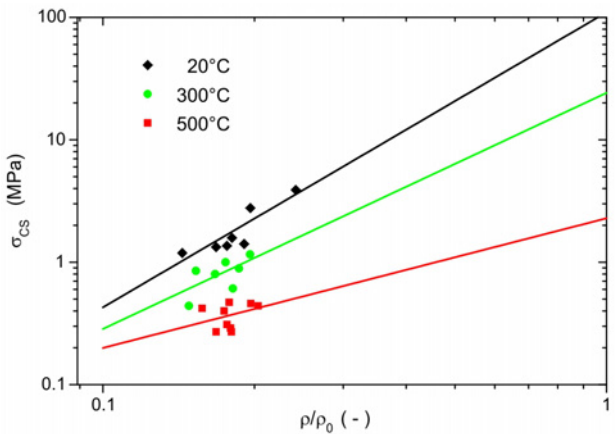

Fig. 8. Log-log plot of compression strength vs. density of AlMg1Si0.6 aluminium foams at various temperatures.

response. Therefore the even identical random structure can have different deformation response to the applied load depending on the testing temperature. Further, as the temperature of foam increases the threshold stress for power law breakdown decreases also. Andrews et al. [20] showed in their simulation that the result is an increase of the activation energy with increasing temperature.

This is probably the reason why the characteristic exponent T_f seems to vary with temperature (see Fig. 8 and Table 6) when the density dependence of the compression strength of aluminium alloy foams at constant temperature is studied. At room temperature, the obtained values for T_f are in relatively good agreement with the theoretical prediction by Arbabi and Sahimi, 2.64 ± 0.3 [23]. Nevertheless, with increasing temperature the characteristic exponent decreases. The highest difference between characteristic exponents T_f at 300 ℃ and room temperature from all investigated alloys was observed for AlSi12 foam, as this brittle alloy at room temperature becomes more ductile at higher temperatures. It must be noted that prior fitting, the values of the ultimate tensile strength of bulk alloys at given temperature were included in the data sets. Unfortunately, no literature data can be found for the ultimate tensile strength of corresponding aluminium alloys at 500 ℃. Therefore low values of T_f with high scatter were observed at 500 ℃.

Summarising, it was confirmed that at given temperature and low applied load, the foam and solid material creep constants (activation energy, power law exponent) ought to be nearly the same regardless of the density. The temperature change of the characteristic exponent values for compression strength indicates further, that when external load and temperature increase significantly, the foam creep constants can vary. This is probably the result of foam struc-

ture: At constant temperature, some cell walls undergo power law breakdown regime and act as removed from the structure, when external load exceeds the certain threshold value. Moreover, the threshold value and the local distribution of stresses within foam structure changes significantly with temperature. As a consequence of this, the compression strength of foam of certain porosity normalised by the strength of matrix alloy is higher at a higher temperature as it is at room temperature. It must be pointed out that from engineering and design points of view, it can be simpler to consider that the characteristic exponent T_f for the compression strength varies with temperature rather than to determine the activation energy and power law creep exponent.

Metal foams are good for the packaging or crash energy absorption purposes, due to their cellular structure that leads to the existence of the plateau region on the compression stress-strain curve and due to their metallic character that enables high plateau strength. The amount of absorbed energy W per unit volume V up to given strain ε is an area under stress-strain curve:

$$W(\varepsilon)/V = \int_0^{\varepsilon} \sigma(\varepsilon)\,\mathrm{d}\varepsilon. \quad (4)$$

The plateau region is the most important part of the foam stress-strain curve for the energy absorption purposes. It starts at strain at compression strength ε_{cs} when the macroscopic failure of foam occurs and ends at densification strain ε_D when all principal pore layers within foam structure are already crushed. Within this region, the energy is absorbed by the subsequent structural collapse (buckling, yielding or crushing) of pore layers approximately perpendicular to the applied load. This effect enables very effective energy absorption at nearly constant load.

For the simplification of general equation (4), it can be considered that the plateau stress is constant. Then, after integrating of Eq. (4) this simplification leads to

$$W(\rho,T)/V \approx \sigma_{cs}(\rho,T)\times[\varepsilon_D(\rho,T) - \varepsilon_{cs}(\rho,T)], \quad (5)$$

where the compression strength of foam $\sigma_{cs}(\rho,T)$ was used instead of plateau stress. This complex dependence is in general non-linear and with increasing temperature, the amount of absorbed energy decreases significantly (Fig. 9). Principally, the absorbed energy at high temperature is lower due to the lower compression strength, which temperature dependence can be successfully modelled using Eq. (3). The length of the strain range between densification strain and strain at compression strength is very important when there is prescribed the amount of impact energy to absorb and maximal peak force acting on protected object. Often

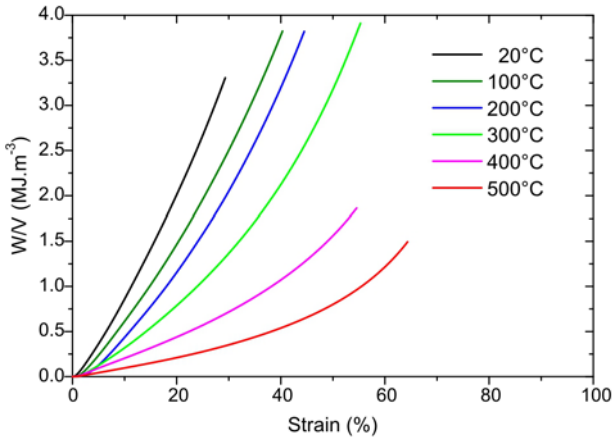

Fig. 9. Temperature dependence of absorbed energy per unit volume versus strain for AlSi12 aluminium foam at constant density 730 kg m^{-3}.

the foam of some density can be suitable thanks to its plateau strength, but the deceleration path is too short, and in the densification region the force acting on the system exceeds the maximal safe load on the object. Thus to model the energy absorption of metallic foam, it is necessary to look also after the density and temperature dependence of both strains.

The deformation of foam's cell walls starts from the early stages of compression loading, and the degree of plasticity depends predominantly on the foam composition and density. Since the cellular structure possesses the cell wall thickness distribution and various loading conditions (tension, compression, bending, shearing) in individual cell walls, the cell walls yield or break locally when local stress grows over critical stress level for an individual cell wall. When the long-range correlation among already failed cell walls takes place, the macroscopic failure of foam sample occurs within the so-called weakest link. At this point of the structure evolution, the compression strength of the sample is measured, and the strain at compression strength is determined.

Generally, within the validity of Hooke's law, the modulus of elasticity of metals decreases with increasing temperature. As a result, strain at constant stress increases significantly with temperature. The effect also occurs inside the cell walls of aluminium foams. Therefore we have observed for brittle AlSi12 foams an increase of strain at compression strength with temperature (Fig. 10). Astoundingly it is not the major effect: The results show that the ductile foams prefer almost temperature-independent strain at compression strength. Also, in this case, the foam composition is very important: The pure Al99.5 foam possesses a higher value of the strain at compression strength at a lower density as the wrought AlMg1Si0.6 foam (see Fig. 10). The obtained results can be probably ex-

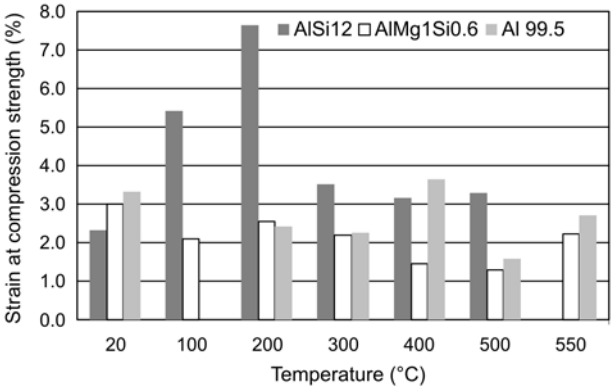

Fig. 10. The temperature dependence of the strain at compression strength (ε_{cs}) of aluminium alloy foams (Al99.5 – density 310 kg m^{-3}, AlSi12 – density 730 kg m^{-3}, AlMg1Si0.6 – density 410 kg m^{-3}).

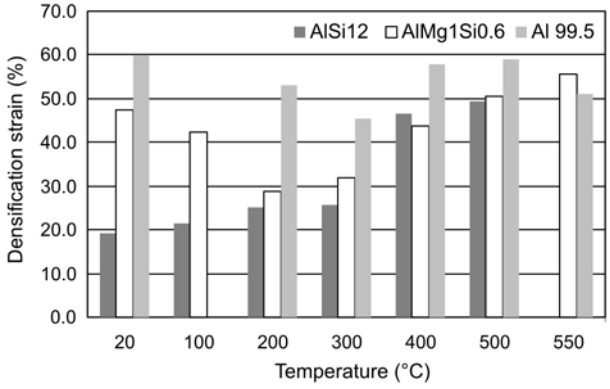

Fig. 11. The temperature dependence of the densification strain (ε_D) of aluminium alloy foams (Al99.5 – density 310 kg m^{-3}, AlSi12 – density 730 kg m^{-3}, AlMg1Si0.6 – density 410 kg m^{-3}).

plained as follows: Elasticity of foam matrix material enables cell walls to reach higher relative deformation. Further, the deformation of the foam is influenced by the decreasing value of the compression strength with increasing temperature. But the key role plays plasticity of ductile foam sample that starts at lower sample strain: The local stress within foam structure grows over critical stress level earlier due to lowered value of the critical stress of matrix alloy with temperature. Furthermore, at high temperatures also shear mode is present instead of pure compression/tension failure modes and probably also Poisson's ratio of foam can change. So plasticity works against elasticity and as a result the strain at compression strength of ductile foams is almost temperature independent. Proposed explanation of the problem can be demonstrated using AlSi12 foam: Up to 200 ℃, the foam undergoes predominantly elastic-brittle deformation. Above 200 ℃, the foam becomes ductile, and the plastic deformation prevails from the early stages of loading. Therefore above this temperature strain at compression strength is almost temperature independent also for this cast aluminium alloy.

The densification strain ε_D is a point at which all pore layers within foam structure are already crushed and partially deformed. After this point, the stress within foam increases significantly. The densification strain is usually determined by the sharp decrease of the energy absorption efficiency on efficiency-strain curve [24, 25]. Nevertheless, it is often very difficult to determine any sharp decrease precisely. For that reason, the determined values of the densification strain possess a usually higher degree of uncertainty in comparison with strain at compression strength and high scatter of data can be observed. This can be the reason, why AlMg1Si0.6 alloy foam shows the minimum of densification strain between 200–300 ℃ in Fig. 11. However, it is obvious that increased plasticity of brittle AlSi12 foam also leads to the significant increase in densification strain with temperature.

The length of plateau region of foam depends significantly on the alloy composition, i.e., brittleness or ductility of matrix aluminium alloy. How does it work? The brittle foam fails at first at the weakest link, and then subsequently via neighbouring pore layers by crack growth and brittle failure, while the rest of the sample remains almost untouched because it is mainly within elastic region. High compression strength of alloy prevents subsequent full densification of already crushed cell walls. Thus after all pore layers are already crushed, there is still some free volume left within compressed pores. Further, this free volume has to be fully compressed within densification region. Therefore the immediate increase of the stress with strain is a bit slower, as it is in the case of ductile foams. On the contrary, ductile foams fail at first at the weakest link, but subsequently, the whole structure is deformed with predominant plastic deformation of the second weakest region of the sample, which is not usually in the neighbourhood of the previously deformed layer. Lower compression strength of alloy enables higher subsequent densification of already crushed cell walls. Thus after all pore layers are already crushed, left free volume within compressed pores is significantly lower than in the case of brittle foam. The plasticity of the alloy also leads to the higher lateral expansion of the whole sample, not only crushed pore layers.

Further, it is generally accepted that the densification strain depends linearly on the relative foam density [13] at room temperature:

$$\varepsilon_D(\rho) = 1 - A\frac{\rho}{\rho_s}, \tag{6}$$

where A is a material constant and is usually 1.4–3 for aluminium foams.

Table 7. Linear regression L_p = a + bT for aluminium alloy foams. a and b are fitting constants, R' is correlation coefficient, and P is the number of data points, constant $a = -E - F\frac{\rho}{\rho_s}$, according to Eq. (8), represents the theoretical length of plateau at zero temperature, $b = \left(1 - A\frac{\rho}{\rho_s}\right)/T_0$, where T_0 = 293 K is room temperature

Alloy	Density (kg m^{-3})	a	b	R'	P	A
AlSi12 foam	**730***	–0.0927 ± 0.0911	0.00069 ± 0.00017	0.9020	6	**2.95**
	520	0.1600 ± 0.0740	0.00040 ± 0.00013	0.7665	9	4.58
	440	0.2479 ± 0.0608	0.00033 ± 0.00011	0.7640	9	5.54
AlMg1Si0.6 foam	530	0.2037 ± 0.0485	0.00022 ± 0.00008	0.8013	6	4.77
	470	0.2199 ± 0.0626	0.00036 ± 0.00010	0.7548	12	5.14
	410*	0.2732 ± 0.1067	0.00023 ± 0.00018	0.4608	8	**6.14**
Al99.5 foam	470	0.4047 ± 0.0355	0.00008 ± 0.00006	0.4129	10	5.61
	370	0.4659 ± 0.0385	0.00006 ± 0.00007	0.3446	9	7.17
	310*	0.5373 ± 0.0844	–0.00003 ± 0.00013	–0.1212	6	**8.79**

*Data in the range of 20–550 °C.
**Other results are linear regression constants for data at 20, 300 and 500 °C.

Finally, we can model the dependence of the length of plateau region for ductile aluminium foams and brittle foams above 300 °C. Generally, both strains depend almost linearly on the density at a constant temperature. Therefore the following density dependence of length of plateau at room temperature

$$L_P(\rho, 293\,\mathrm{K}) = \left(1 - A\frac{\rho}{\rho_s}\right) - \left(E + F\frac{\rho}{\rho_s}\right) \qquad (7)$$

can be considered. From Eq. (7) it is evident that with the decreasing density, the plateau length increases at room temperature. As was mentioned previously, the strain at compression strength (macroscopic failure of the sample) is nearly temperature independent at a constant density for ductile foam. A further requirement is that the model ought to give Eq. (7) at room temperature. These facts enable to model plateau length dependence on temperature in simple scaling form

$$L_P(\rho, T) = \left(1 - A\frac{\rho}{\rho_s}\right)\frac{T}{T_0} - \left(E + F\frac{\rho}{\rho_s}\right), \qquad (8)$$

where room temperature is used as normalised temperature T_0. However, as can be seen from Table 7, this model gives relatively high values of constant A which characterises the dependence of densification strain on density. This indicates that the proposed model is an only linear approximation of real events, which are principally non-linear.

Also in this data representation, it was experimentally observed that the length of plateau region for pure aluminium and wrought aluminium alloy foams is nearly unchanged at different temperatures, due to the plasticity of used alloy. The increased plasticity for brittle AlSi12 alloy foams can also be observed as the length of plateau possesses significant increase above 300 °C at high density (see Figs. 12, 13).

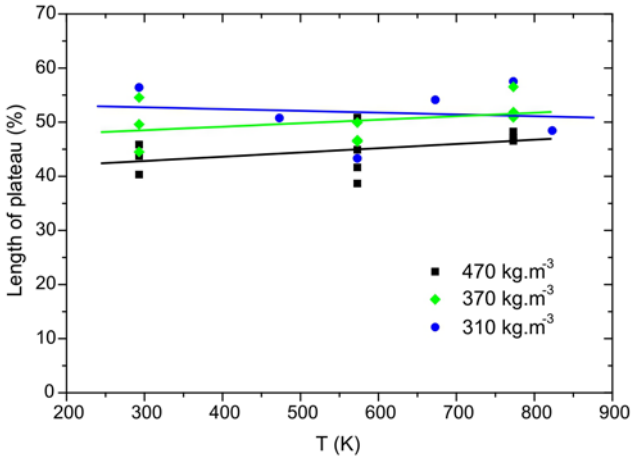

Fig. 12. Temperature dependence of plateau length for Al99.5 aluminium foams.

4. Conclusions

The temperature dependence of compression behaviour: strength and energy absorption capacity of PM aluminium foams (pure Al99.5, wrought AlMg1Si0.6 alloy and casting AlSi12 aluminium alloy) in the temperature range 20–550 °C was systematically studied.

It can generally be concluded that the rise in temperature results in a decrease of the compression strength and energy absorption, and in an increase of densification strain and plateau length.

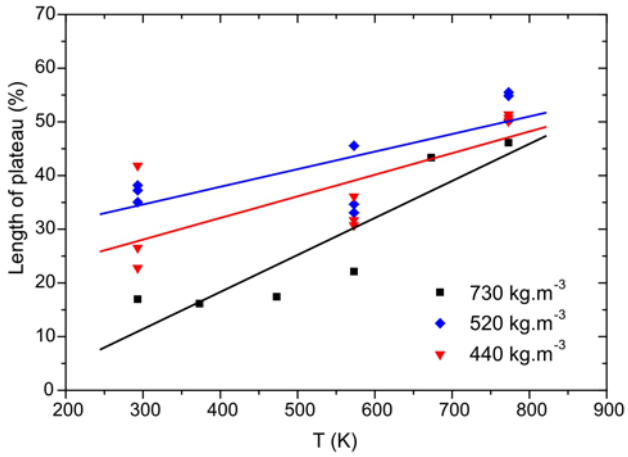

Fig. 13. Temperature dependence of plateau length for AlSi12 aluminium foams.

Al99.5 and AlMg1Si0.6 foams show purely ductile rupture of the cell walls from the room temperature. AlSi12 foam usually fails by brittle fracture up to 200 ℃ and by a mixture of brittle fracture and ductile tearing above 200 ℃. It implies that with increasing temperature the ductile features prevail for this alloy. The smoothing of the serrated stress-strain curve for AlSi12 foams with temperature confirms this.

The compression strength of aluminium foams decreases significantly for all types of used alloys with temperature. It was experimentally confirmed, that heating up above 300 ℃ diminishes the strength differences between aluminium alloy foams. From a technological point of view, this enables to form foam samples to net shape at much lower applied force.

The dependence of compression strength on foam density and temperature can be successfully modelled using proposed Eq. (3).

It was confirmed that at given temperature and low applied load, the foam and solid material creep constants (activation energy, power law exponent) ought to be nearly the same regardless of the density. However, both values can change with temperature: At constant temperature, some cell walls undergo power law breakdown regime and act as removed from the structure, when external load exceeds the certain threshold value. Moreover, the threshold value and the local distribution of stresses within foam structure changes significantly with temperature. It must be pointed out, that for engineering and design of foams, it can be simpler to consider that the characteristic exponent T_f for the compression strength varies with temperature rather than to determine the activation energy and power law creep exponent.

The strain at compression strength (macroscopic failure of the sample) is nearly temperature independent or even decreases at constant density depending on aluminium alloy. It is probably the result of increased plasticity (low value of critical stress of matrix alloy and high local deformation to failure), which increases the lateral foam expansion with temperature. Unfortunately, for this reason, the high-temperature forming is limited only to low deformation strains.

It was further observed that the density dependence of strain at compression strength remains linear also at high temperatures.

It can be concluded that the absorbed energy per unit volume of aluminium foams decreases with increasing temperature significantly due to the decrease in the value of plateau/compression strength. The increase of the plasticity of foam giving longer plateau length with increasing temperature acts against this. However, the second effect is less pronounced and is technologically important only when extremely high deformation length (deceleration path) is required.

The higher values of a material constant A for densification strain density dependence of 3–8.8 than usual values of 1.4–3 for aluminium foams [13] were observed.

It was also confirmed, that by choosing proper matrix alloy composition and relative density the foam can be tailored to give the best combination of properties for given protective casing also at higher temperatures.

Acknowledgements

The financial support of Alulight International, Ranshofen, Austria is gratefully acknowledged. This work was also partially supported by the Slovak Grant Agency under contract VEGA 2/0065/16, Slovak Research and Development Agency under contract APVV-0692-12 and bilateral agreement SK-RO-0014-12 and UPT 653/2013.

One of the authors, J. K., thanks to IMMM SAS, Bratislava, Slovakia and Royal Society, London, UK for the financial support of his stay in the UK. He would also like to thank V. Gergely, T. W. Clyne and F. Simančík for their extraordinary support in creating this article.

References

[1] Banhart, J.: Progress in Materials Science, *46*, 2001, p. 559. doi:10.1016/S0079-6425(00)00002-5

[2] Kováčik, J., Simančík, F., Kovove Mater., *42*, 2004, p. 79.

[3] Marsavina, L., Kováčik, J., Linul, E.: Theor. Appl. Frac. Mec., *83*, 2016, p. 11. doi:10.1016/j.tafmec.2015.12.020

[4] Kováčik, J., Jerz, J., Mináriková, N., Marsavina, L., Linul, E.: Frattura ed Integrità Strutturale, *36*, 2016, p. 55; doi:10.3221/IGF-ESIS.36.06

[5] Orovčík, Ľ., Nosko, M., Kováčik, J., Dvorák, T., Štěpánek, M., Simančík, F.: Kovove Mater., *54*, 2016, p. 463.

[6] Thornton, P. H., Magee, C. L.: Metall. Trans. A, *6*, 1975, p. 1801. doi:10.1007/BF02642310

[7] García-Moreno, F.: Materials, *9*, 2016, p. 85. doi:10.3390/ma9020085
[8] Aly, M. S.: Mater. Lett., *61*, 2007, p. 3138. doi:10.1016/j.matlet.2006.11.046
[9] Hakamada, M., Nomura, T.: J. Mater. Res., *20*, 2005, p. 3385. doi:10.1557/jmr.2005.0415
[10] Wang, P., Xu, S., Li, Z., Yang, J., Zheng, H., Hu, S.: Mater. Sci. Eng. A, *599*, 2014, p. 174. doi:10.1016/j.msea.2014.01.076
[11] Sahu, S., Goel, M. D., Mondal, D. P., Das, S.: Mater. Sci. Eng. A, *607*, 2014, p. 162. doi:10.1016/j.msea.2014.04.004
[12] Liu, J., Qu, Q., Liu, Y., Li, R., Liu, B.: J. Alloys Compd., *676*, 2016, p. 239. doi:10.1016/j.jallcom.2016.03.076
[13]. Gibson, L. J, Ashby, M. F.: Cellular Solids: Structure and Properties. 2nd Edition. Cambridge, Cambridge University Press 1997.
[14] Sugimura, Y., Meyer, J., He, Y., Bart-Smith, H., Grenested, J., Evans, A. G.: Acta Mater., *45*, 1997, p. 5245. doi:10.1016/S1359-6454(97)00148-1
[15] Markaki, A.: Mechanical Behaviour of Layered Metal Foam/Ceramic Composites. [PhD. Thesis]. Cambridge, Cambridge University 2000, p. 95.
[16] Simančík, F., Kováčik, J., Sedliaková, N.: In: Proceedings of Powder Metallurgy World Congress and Exhibition. Shrewsbury, EPMA 1998, p. 245. ISBN 1 899072 09 8
[17] Banhart, J., Baumeister, J.: J. Mater. Sci., *33*, 1998, p. 1431. doi:10.1023/A:1004383222228
[18] Weiss, M. J., Mataya, M. C., Thompson, S. W., Matlock, D. K.: In: Proceedings of Superalloy 718 – Metallurgy and Applications. Ed.: Loria, E. A. Warrendale, TSM 1989, p. 135.
[19] Mecking, H., Styczynski, A., Estrin, Y.: Proceedings of the 8th International Conference on the Strength of Metals and Alloys. Eds.: Kettunen, P. O., Lepistö, T. K., Lehtonen, M. E. Oxford, Pergamon Press 1998, p. 989. ISBN: 978-0-08-034804-9
[20] Andrews, E. W., Huang, J.-S., Gibson, L. J.: Acta Mater., *47*, 1999, p. 2927. doi:10.1016/S1359-6454(99)00161-5
[21] Lapin, J., Delanney, F.: Metall. Trans. A, *26*, 1995, p. 2053. doi:10.1007/BF02670677
[22] Frost, H. J., Ashby M. F.: Deformation Mechanism Maps. Oxford, Pergamon Press 1982.
[23] Sahimi, M., Arbabi, S.: Phys. Rev. B, *47*, 1993, p. 713. doi:10.1103/PhysRevB.47.713
[24] Florek, R., Simančík, F., Nosko, M., Harnušková, J.: Powder Metall. Progr., *10*, 2010, p. 207.
[25] Linul, E., Şerban, D. A., Marsavina, L., Kováčik, J., Sadowski, T.: P. Romanian Acad. A, 2016. Accepted (in press).